ISCoS The International Spinal Cord Society

www.nature.com/sc

ARTICLE

Check for updates

Low-intensity pulsed ultrasound partially reversed the deleterious effects of a severe spinal cord injury-induced bone loss and osteoporotic fracture healing in paraplegic rats

Ariane Zamarioli[1]✉, Mariana M. Butezloff[1], João P. B. Ximenez[2] and José B. Volpon[1]

PURPOSE: To evaluate the effects of low-intensity pulsed ultrasound (LIPUS) on the quality of femoral fracture callus formation in rats with severe osteoporosis secondary to spinal cord injury (SCI).

METHODS: Forty-five male rats were equally divided into three groups: the Sham group underwent sham surgery for SCI followed by surgery for femoral fracture on day ten post-spine surgery; the SCI group sustained a complete transection of the spinal cord and a femoral fracture ten days post-SCI; and the SCI group treated with ultrasound (SCI + US), which also sustained a femoral fracture on day ten post-SCI, concomitant with daily application of LIPUS at the fracture site.

RESULTS: At the non-fractured tibias, LIPUS counteracted the SCI-induced bone loss by normalizing the osteoblastic-related gene expression, decreasing resorptive area, increasing trabecular area, and decreasing RANK and RANK-L-positive areas, which resulted in higher cortical volume and stronger tibias. Likewise, LIPUS was effective at restoring bone fracture healing in SCI rats; by promoting endochondral ossification, increasing collagen deposition and OPG-positive-area, decreasing resorptive area, which led to higher density and improved microarchitecture, ultimately resulting in stronger fracture callus.

CONCLUSION: At the tibias, LIPUS counteracted the SCI-induced bone loss effects by simultaneously increasing bone formation and decreasing bone resorption. We also evidenced the osteogenic effects of LIPUS at partially restoring the endochondral ossification during callus formation, leading to a newly formed tissue with improved microarchitecture and mechanical integrity. Therefore, LIPUS may be an efficient and non-invasive approach to prevent bone loss and osteoporotic fracture in SCI individuals.

Spinal Cord (2023) 61:145–153; https://doi.org/10.1038/s41393-022-00863-1

INTRODUCTION

Spinal cord injury (SCI) represents a devastating event in an individual's life. SCI greatly affects several organs and systems, resulting in neurogenic bladder [1], neurogenic bowel dysfunction [2], and impairments in the respiratory [3], cardiovascular [4], and tegumentary systems [5]. The locomotor system is particularly affected, showing different clinical pictures of paresis, paralysis, and loss of sensitivity, secondarily resulting in deformities, pressure ulcers formation, joint stiffness, and changes in bone quality and structure, which are manifested by micro- and macro-deterioration, loss of bone mass, fragility, and pathological fractures [6].

The sequelae of SCI include fractures, which are orthopedically and clinically characterized by severe osteoporosis and bone fragility, respectively, resulting in the difficulty of using implants for further fixation. Thus, efforts have been made to find alternatives to improve the bone quality and the consolidation of fractures in SCI individuals. One of the main physical resources is the low-intensity pulsed ultrasound (LIPUS). Experimental and clinical studies have reported the benefits of its use on the bone healing process [7]. Experiments have shown that LIPUS can accelerate the healing of osteoporotic fractures in ovariectomized rats with delayed mineralization and altered biochemical properties [8]. However, previous studies have not established the benefits of low-intensity ultrasound therapy on bone fractures affected by severe osteoporosis, such as in cases of SCI. This study aimed to evaluate the effect of LIPUS application on experimental fracture healing in rats with SCI. We hypothesized that LIPUS plays an osteogenic effect at improving the quality and quantity of the newly formed bone callus.

METHODS

All experimental procedures were approved by the Institution's Animal Experimentation Ethics Committee (Protocol no. 199/2015). We used 6-week-old male Wistar rats, with a body mass between 180 g and 200 g. The daily care followed the guidelines for the care and use of laboratory animals and the entire animal study was conducted following the 3Rs principle [9], and the guide for the care and use of laboratory animals [10]. After three days of acclimation, the animals ($n = 54$) were randomly distributed into three experimental groups ($n = 18$/group): 1- Sham: sham procedure for SCI, and femur fracture ten days later; 2- SCI, and; 3- SCI-treated group with ultrasound application (SCI + US).

Spinal cord injury

The animals were anesthetized with intramuscular administration of xylazine, 7.5 mg/kg, and ketamine, 60 mg/kg. The SCI procedure was

[1]Ribeirão Preto Medical School, University of São Paulo, Sao Paulo, Brazil. [2]School of Pharmaceutical Sciences of Ribeirao Preto - University of São Paulo, Sao Paulo, Brazil. ✉email: arianezamarioli@usp.br

Received: 8 December 2021 Revised: 3 October 2022 Accepted: 6 October 2022
Published online: 20 October 2022

performed according to routine surgical techniques for asepsis and antisepsis, which has been previously detailed [11]. In brief, the laminae at the T10 level were resected, and the spinal cord was completely sectioned. Buprenorphine, 0.03 mg/kg was administered intramuscularly twice daily, and 10 mL of Ringer lactate was administered subcutaneously for 5 days to prevent dehydration. The bladder was emptied twice a day by careful digital pressure on the lower abdomen. The same investigator daily examined the rats following spinal cord injury and sham surgery, which consisted of postoperative care for general health assessment (including signs of stress), skin examination, neurological and locomotor functional assessment to confirm immediate and persistent complete sublesional paralysis, with no gain of function.

Bone fracture

Ten days after the surgery for SCI, the diaphyseal region of the right femur was fractured, under anesthesia, using a blunt blade guillotine especially made for this purpose [11, 12]. Internal fixation was performed with a 1.0-mm Kirschner wire. Radiography was performed at days 0, 7, and 14 after the surgery for fracture follow-up. At the time of surgery, subjects with comminuted fractures of more than three fragments or with long oblique fractures were excluded.

Low-intensity pulsed ultrasound

LIPUS application started 36 h after the fracture production. It was administered five times a week for 20 min each session, with the transducer positioned on the lateral thigh over the fracture site. The parameters were as follows: frequency of 1.5 MHz, a pulse width of 200 µs, wave amplitude (peak to peak) of 25 V, and intensity of 30.0 mW/cm^2 (EESC-USP, Brazil) [13].

Microarchitecture of the bone callus

The microarchitecture of the bone callus was analyzed using a microtomography (µCT) (SkyScan 1272v2; Bruker-microCT, Kontich, Belgium). The following parameters were assessed: entire bone callus volume (BCa.V, in mm^3); woven bone fraction, expressed as a percentage of the callus volume and interpreted as the callus mineralization (BCa.BV/TV, in %); callus porosity (BCa.Po, in %); and tissue mineral density (TMD, g/mm^3); newly formed trabecular thickness (Tb.Th, in mm), separation (Tb.Sp, in mm), number (Tb.N, in 1/mm); and connectivity density (Conn.D, in 1/mm^3). The nomenclature used is in accordance with the American Society for Bone and Mineral Research [14], but it should be highlighted that these parameters are for standard bone. However, while there are no specific parameters for fracture healing, they are commonly adapted for assessing callus quantity and quality [15, 16].

Bone densitometry

Dual-energy x-ray absorptiometry (DXA) was performed with a Lunar densitometer DPX-IQ (Lunar; software version 4.7e, GE Healthcare, Chalfont St. Giles, United Kingdom). The entire callus was selected to determine the bone mineral density (BMD, in g/cm^2), the bone mineral content (BMC, in g), and the area (region of interest, in cm^2). The scanning reproducibility (4%) was assessed by the root mean square coefficient of variation.

Mechanical testing

After densitometry and µCT, the fractured femurs underwent a mechanical low-speed torsion test on the Instron 55MT machine (USA) and tibias were tested by three-point-bending axial test.

Microscopy

5-µm axial sections were stained with hematoxylin-eosin (H&E), Masson's trichrome, tartrate-resistant acid phosphatase (TRAP), and picrosirius red. Masson's trichrome staining was used to quantify the trabecular bone and bone callus using the AxioImager Z2 (Zeiss, Germany). The blue color demarcated the entire area corresponding to the trabecular bone, expressed as a proportion of the bone area by the total area (B.Ar/Tt.Ar), imaged with a magnification of 50×. Collagen was quantified in sections stained with Picrosirius red, using Axiovision. The area was expressed as a percentage of the collagen area by the total area (Col.Ar/Tt.Ar, %), imaged with a magnification of 50×. TRAP staining was used to calculate the number of osteoclasts, with a magnification of 100×, in which the red color demarcated the osteoclast areas, and the TRAP-positive area was measured as a percentage of the entire callus area at the fractured femur (%). For immunohistochemistry, the tissues were incubated with primary antibodies for osteoprotegerin (OPG; sc8468, polyclonal anti-goat, Santa Cruz, Dallas-TX, USA), the receptor activator of nuclear factor kappa-B (RANK; sc9072, polyclonal anti-rabbit, Santa Cruz, Dallas-TX, USA), and the receptor activator of nuclear factor kappa-B ligand (RANKL; sc7628, polyclonal anti-goat, Santa Cruz, Dallas-TX, USA). Positives immunostaining for OPG, RANK, and RANKL were quantitatively assessed with the Axiovision (Zeiss, Germany) software. These were expressed as the proportion of the protein expression area to the total area (B.Ar/Tt.Ar, %).

RNA isolation and real-time PCR assessment

Total RNA was extracted from both the fracture callus and the non-fractured tibias ($n = 6$/bone/group) using an SV Total RNA Isolation System (Promega, Madison, Wisconsin, USA). Complementary DNA (cDNA) synthesis was performed with 1 µg RNA using High-Capacity cDNA Reverse Transcription Kit (Applied Biosystems, Foster City, CA, USA). TaqMan® gene expression assays (Applied Biosystems) were used for quantifying collagen type 1, alpha 2 (Col1a1), runt-related transcription factor 2 (Runx2), and osterix (Osx) expression by quantitative PCR on a StepOnePlus PCR machine (Applied Biosystems). Data were normalized to the expression of the reference gene GaPDH, which gave consistent average values in this study. Samples were run in duplicates, and relative expression was calculated using 2−ddCT, and the ddCt was calculated as dCt[goiSCI - refSCI] - dCt[goiSham - refSham], where goi are the genes of interest and ref is the reference gene. For descriptive and statistical analyses, ddCT was applied as a continuous variable. The mean for each gene of interest for the sham group was calculated and used to normalize the other groups to indicate how SCI and fracture regulate expression levels.

Statistical analysis

All statistical analyses were performed using the RStudio (RStudio, Inc, USA) software. Continuous variables were expressed as mean and standard deviation (SD). The Shapiro-Wilk normality test was performed, and the ANOVA test was used to compare data between groups. Tukey's post-hoc test was used for multiple comparisons between groups. The significance level was set at $p < 0.05$.

RESULTS

Post-operative complications are known to be common in SCI rats, whose mortality rate increased by the addition of femoral fractures to these animals, as previously described [11]. No losses occurred due to the LIPUS therapy. Although the animals with SCI showed a 26% decrease in body mass by the end of the experiment compared to the shams ($p < 0.001$), there was no significant difference in body mass between the SCI and SCI + US groups.

LIPUS significantly counteracted the SCI-induced downregulation of osteoblastic-related genes in non-fractured bones

As previously published [11], SCI significantly downregulated the expression of osteoblastic-related genes ($p = 0.03$ for Cola1 and Osx and $p = 0.07$ for Runx2), impairing bone formation at several stages of osteoblast differentiation. LIPUS significantly increased the expression of Col1a1 at the tibias when compared to the non-treated SCI rats ($p = 0.02$, Fig. 1A). No significant differences were detected between SCI-treated rats with LIPUS and the sham group at the tibias ($p = 0.74$ for Cola1, $p = 0.34$ for Osx, and $p = 0.60$ for Runx2, Fig. 1A). Although osteoblastic-related gene expression was severely downregulated by SCI at the non-fractured bone, we did not detect any changes at the fracture callus in SCI rats compared to control animals ($p = 0.9$ for Cola1, $p = 1.0$ for Osx and $p = 0.9$ for Runx2, Fig. 1B). LIPUS significantly increased the expression of Col1a1 by 85% at the femoral callus when compared to the non-treated SCI rats ($p = 0.02$, Fig. 1B). Furthermore, an 64% non-significant increase was noted in the SCI + US group when compared to the SCI for the expression of RUNX2 ($p = 0.36$, Fig. 1B). No significant differences were detected between SCI-treated rats with LIPUS and the sham group at the femoral callus

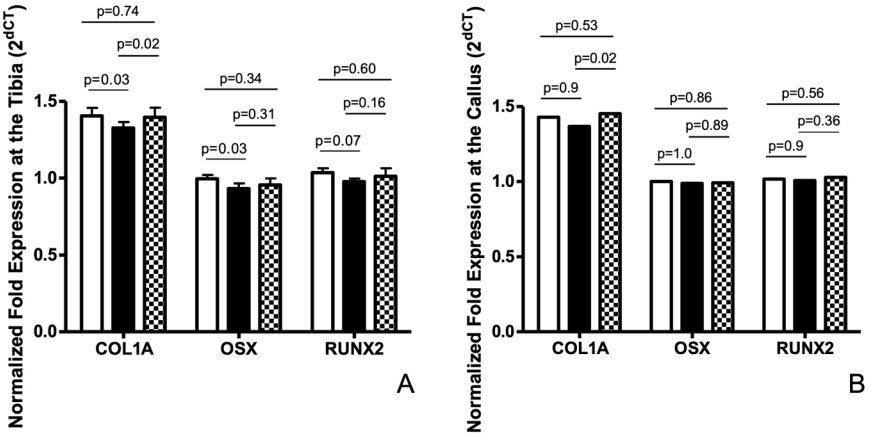

Fig. 1 Gene expression in non-fractured tibias and in femoral calluses. Osteoblastic-related genes at the non-fractured tibias were significantly decreased in the SCI group when compared to the Shams, whose reductions were counteracted by LIPUS treatment (**A**). Conversely, these genes were not altered at the fracture callus (**B**). Values were normalized to GaPDH expression. Sham; SCI spinal cord injury group, SCI + US spinal cord injury group with low-intensity pulsed ultrasound, Col1A collagen type 1, alpha 2, OSX osterix, RUNX2 runt-related transcription factor 2.

($p = 0.53$ for Cola1, $p = 0.86$ for Osx, and $p = 0.56$ for Runx2, Fig. 1B).

LIPUS partially restored bone cells microenvironment and remodeling activity in SCI rats at the intact tibia and femoral callus

Our TRAP staining sections revealed a significant 71% increase in the resorption activity at the non-fractured tibias in the SCI rats compared to the shams by measuring TRAP-positive area ($p < 0.02$, Fig. 2A), demarcated by red color osteoclasts and pointed by green arrows (Fig. 2B). Conversely, LIPUS significantly decreased the resorption area by 41% compared to the SCI rats without treatment ($p < 0.02$, Fig. 2A) with values compatible to those noted in the Sham rats ($p = 0.13$, Fig. 2A). We detected a significant 60% increase at the tibial trabecular area in LIPUS-SCI-treated rats compared to the non-treated paraplegic rats ($p = 0.009$, Fig. 2C), which can be noted in Fig. 2D where the trabecular bone is blue colored by Masson staining. This increase fully restored its values to those compatible with the shams ($p = 0.13$, Fig. 2C), which were previously decreased by the SCI ($p = 0.0001$ versus Sham, Fig. 2C). Similarly, total collagen deposition at the non-fractured bone was significantly decreased in the SCI rats compared to the Shams ($p = 0.024$, Fig. 2E), which is shown in Fig. 2F. Although not significantly, LIPUS increased total collagen deposition in the treated SCI rats by 99% ($p = 0.14$) compared to the non-treated paraplegic rats, reaching levels comparable to the Shams ($p = 0.62$, Fig. 2E). Our immunohistochemistry analysis confirmed the unbalanced bone turnover evidence by our stained histological sections. As previously published, the SCI group showed a significant 273% increase in the RANK-positive area (2.35 ± 0.20% versus 0.63 ± 0.14%, respectively, $p < 0.0001$) and 112% in the RANKL-positive area, compared to the shams (1.95 ± 0.42% versus 0.92 ± 0.94%, respectively, $p = 0.002$). LIPUS significantly decreased the RANK-positive area by 48%, $p = 0.0001$, and tended towards a reduction in the RANK-L-positive area by 21%, $p = 0.08$, compared to the non-treated SCI rats. Although a significant difference was not found between the groups, the OPG-positive area was 16% lower in the SCI group compared to the control (2.17 ± 0.36% versus 2.59 ± 0.99%, respectively, $p = 0.37$), and 72% higher in the LIPUS group versus SCI ($p = 0.12$, Fig. 2G). Positive immunostaining areas for RANK, RANK, and OPG are pointed by green arrows and illustrate the changes detected statistically (Fig. 2H).

As previously reported, bone healing after sustaining an SCI led to a mainly intramembranous callus formation. The paraplegic rats exhibited calluses with more woven bone and trabeculae than shams, in which we detected an abundant presence of cartilaginous tissue on day 14 post-fracture. Interestingly, LIPUS treatment seems to effectively restore endochondral bone formation by exhibiting a large amount of bone cartilage on day 14 post-fracture. Bony bridges were undetected, and fracture gaps were observed in all groups (Fig. 3A). We detected a significant 131% increase in total collagen deposition at SCI rats' callus compared to the shams ($p = 0.0006$, Fig. 3B), which is illustrated in Fig. 3C and might be related to the mainly intramembranous ossification. Although the total collagen deposition slightly reduced by 20% due to LIPUS treatment compared to the SCI rats ($p = 0.409$), the difference between the SCI + US and the Sham group remained significant ($p = 0.008$, Fig. 3B). Conversely, type 1 collagen deposition was significantly increased by LIPUS treatment compared to the non-treated SCI rats ($p = 0.014$). Likewise, LIPUS significantly decreased the resorptive area compared to the SCI and Sham rats ($p < 0.03$, Fig. 3D, E, demarcated by green arrows), but changes in the TRAP-positive area at the callus were not detected between Sham and SCI rats ($p = 0.99$). Our immunohistochemical analysis revealed significant decreases in the OPG and RANKL-positive areas by 75 and 52%, respectively ($p < 0.001$) in the SCI group compared to sham (Fig. 3F). LIPUS significantly increased the OPG-positive area by 85% ($p = 0.009$) in comparison with the non-treated SCI rats, but remained statistically different from the shams ($p = 0.008$). Although LIPUS slightly increased RANK-L-positive area towards the sham level, a significant difference was detected between the SCI + US and the Sham group ($p = 0.008$, Fig. 3F). No changes were detected among the groups regarding the RANK-positive area. Positive immunostaining areas for RANK, RANK, and OPG are pointed by green arrows and illustrate the changes detected statistically (Fig. 3G).

LIPUS was partially effective at restoring bone callus density in SCI rats

Although LIPUS slightly and non-significantly increased tibial bone mineral density (BMD) by 22% and bone mineral content (BMC) by 9% in SCI rats ($p = 0.24$ and $p = 0.87$, respectively), it did not restore the bone mass loss caused by paraplegia. BMD and BMC were significantly lower in the SCI group when compared to the shams (43 and 70%, respectively, $p = 0.0005$ and $p = 0.0006$, Table 1). Conversely, LIPUS treatment significantly increased BMD at the callus compared to SCI rats (0.13 g/cm^2 versus 0.11 g/cm^2, respectively, $p = 0.04$), which was decreased by paraplegia when

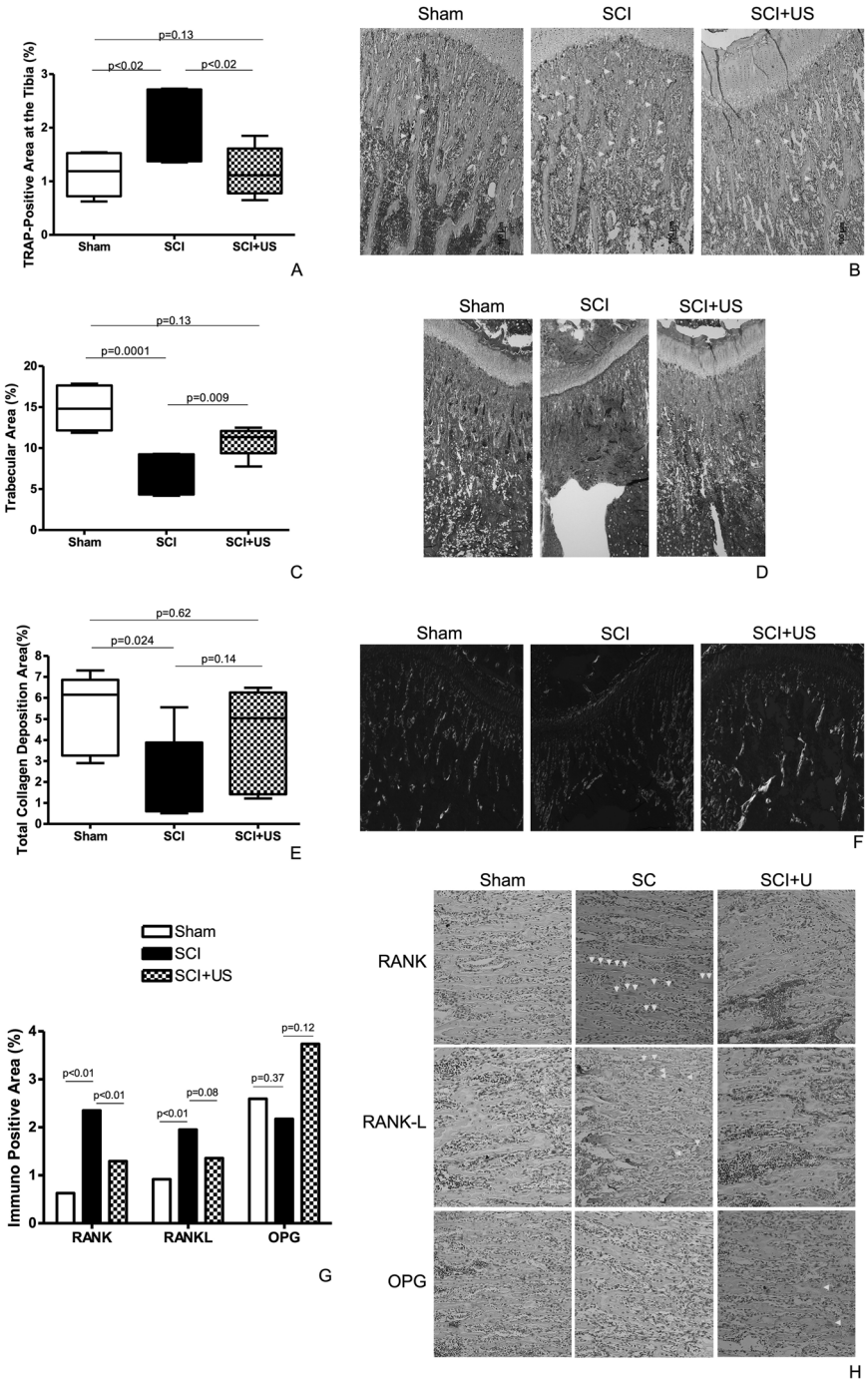

Fig. 2 Bone histology and immunohistochemistry assessment in non-fractured tibias. TRAP-positive area at the tibias was significantly higher in the SCI groups than in the Shams, which was fully restored by LIPUS treatment (**A**). The increased resorption area in the SCI group when compared to the Sham is pointed by green arrows. Furthermore, the TRAP-stained sections also evidence the LIPUS treatment efficacy at reducing TRAP-positive area (arrows point to red color demarcated osteoclasts) when compared to non-treated SCI rats, with magnification of 100× (**B**). In response to the increased osteoclastic activity, trabecular area was significantly reduced in the SCI group in comparison with the Shams, and further increased in the LIPUS-SCI-treated rats (**C**), which may be detected in Masson-stained sections as blue color demarcated areas, magnification of 50× (**D**). Likewise, the SCI rats also exhibited tibias with lower total collagen deposition (**E**), as evidenced by the picrosirius stained slides, with a magnification of 50× (**F**). Corroborating the histological findings of unbalanced bone turnover, SCI group showed higher RANK- and RANK-L-positive area than Shams, which were decreased by LIPUS therapy (**G**). Positive immunostaining areas for RANK, RANK, and OPG are pointed by green arrows. Sham; SCI spinal cord injury group, SCI + US spinal cord injury group with low-intensity pulsed ultrasound, TRAP tetrad-resistant-acid phosphatase, RANK receptor for receptor activator of nuclear factor kappa-B ligand, RANKL receptor activator of nuclear factor kappa-B ligand, OPG osteoprotegerin.

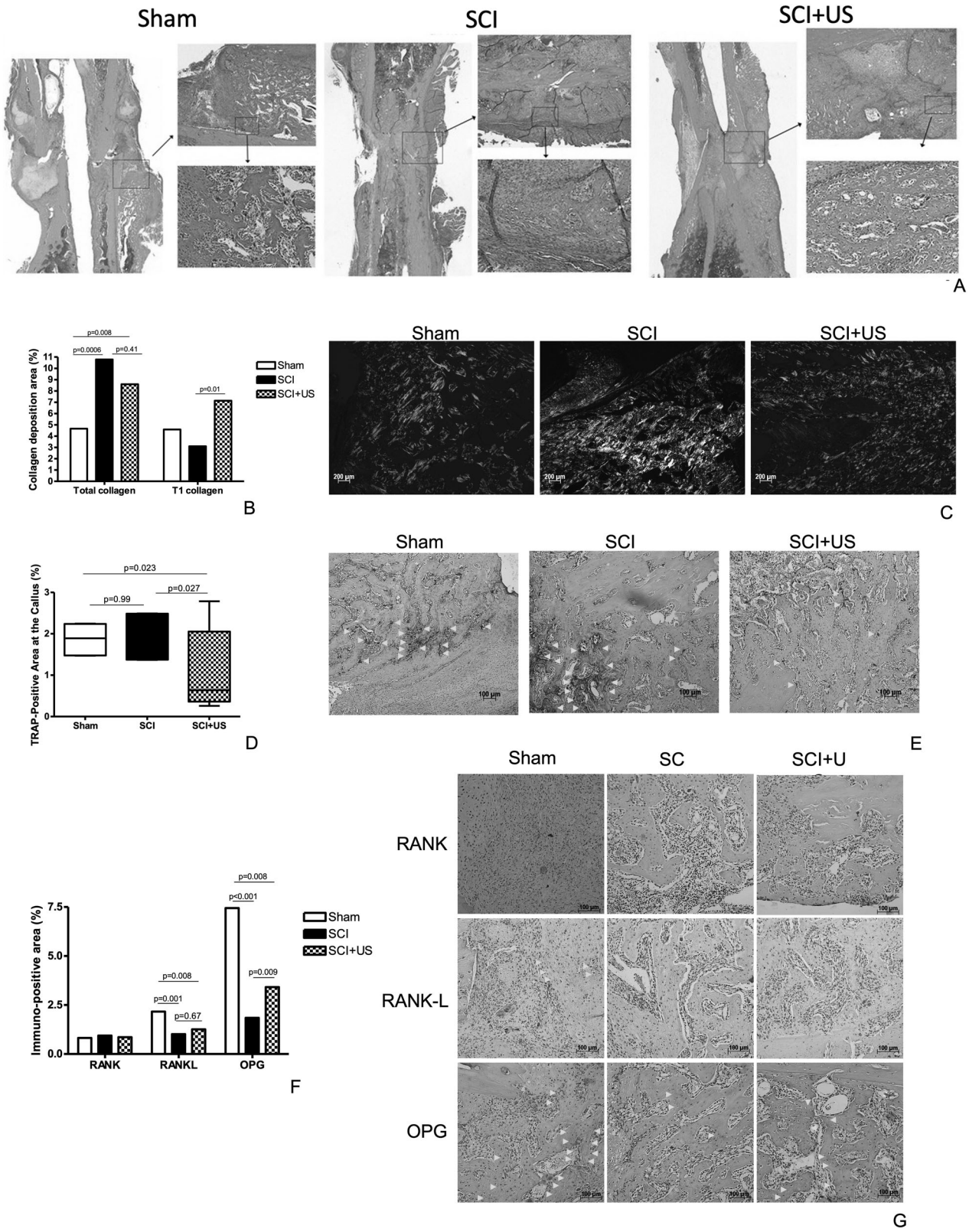

compared to the shams (0.17 g/cm^2, $p = 0.00004$). Similarly, the BMC in the bone callus of the Sham group was significantly higher than in the SCI group (0.07 g and 0.04 g, respectively; $p = 0.02$). Additionally, the BMC values in the SCI + US group (0.05 g) did not significantly differ from those in the Sham or SCI groups ($p > 0.05$). These results indicate that bone calluses were less dense in the spinal cord injured rats than in the shams but increased due to the ultrasound therapy. Additionally, there was no difference in the bone callus area among the groups ($p > 0.05$, Table 1).

Fig. 3 Bone histology and immunohistochemistry assessment in femoral calluses. HE-stained histological images of the fracture callus in all groups, with magnification of 12.5×, 25× and 50×. We suggest a mainly intramembranous ossification in the SCI rats when compared to the Shams. SCI rats exhibit slight cartilaginous tissue and more presence of woven bone and trabeculae than the Shams, which present abundant cartilaginous tissue, woven bone, and few trabeculae in the bone callus. LIPUS was shown to be partially effective at restoring the endochondral ossification, by evidencing more cartilaginous tissue forming the callus (**A**). Corroborating, the fracture calluses in the SCI rats and SCI + US shows higher total collagen deposition than in the Shams (**B** and **C**). Furthermore, the SCI + US rats exhibit higher type 1 collagen deposition at the callus than the non-treated SCI rats (**B**). TRAP-positive area at the callus was significantly lower in the SCI + US groups than in the Shams and non-treated SCI rats (**D**), which can be noted by the green arrows in TRAP-stained slides (red color demarcated osteoclasts), with a magnification of 100× (**E**). SCI groups showed lower RANK-L-positive area than Shams. Likewise, non-treated SCI rats also evidenced lower OPG-positive area than the Shams, which was partially reversed by the US therapy (**F**). Positives immunostaining areas for RANK, RANK, and OPG are pointed by green arrows. Sham; SCI spinal cord injury group, SCI + US spinal cord injury group with low-intensity pulsed ultrasound, TRAP tetrad-resistant-acid phosphatase, RANK receptor for receptor activator of nuclear factor kappa-B ligand, RANKL receptor activator of nuclear factor kappa-B ligand, OPG osteoprotegerin.

LIPUS improved cortical architecture at the tibias and callus microarchitecture and density in SCI rats

SCI led to significant microarchitectural changes at the trabecular and cortical bones of non-fractured bones, as well as at the newly formed bone callus. As of note, SCI significantly decreased BV by 78% ($p = 0.002$), BV/TV by 73% ($p = 0.01$), Tb.N by 68% ($p = 0.03$), and increased Tb.Sp by 83% ($p = 0.02$) compared to the shams, concomitant with trends toward decreases in Tb.Th by 20% ($p = 0.06$), Conn.D by 68% ($p = 0.07$). At the cortical bone, SCI significantly decreased Ct.V by 33% ($p = 0.00004$), Ct.BV/TV by 17% ($p = 0.003$), and TMD by 9% ($p = 0.08$) when compared to controls. Although LIPUS did not significantly modify the changes caused by paraplegia itself at the trabecular bone, it significantly increased cortical volume (27% for CT.V, $p = 0.0003$; 15% for Ct.BV/TV, $p = 0.01$) when compared to the non-treated SCI rats (Table 1).

Although the formation-related microarchitectural parameters (μCT) of the bone callus were lower in the paraplegic animals, LIPUS improved the quality and quantity of the newly formed bone tissue structure. LIPUS induced significant increases in Ca.BV/TV ($p = 0.04$ versus Sham and $p = 0.09$ versus SCI), Tb.Th ($p = 0.03$ versus SCI and $p = 0.05$ versus SCI), Tb.N ($p = 0.0001$ versus Sham and $p = 0.003$ versus SCI), Ca.TMD ($p = 0.02$ versus Sham), and Conn.D ($p < 0.001$ versus SCI and Sham), concomitant with reductions in Tb.Sp ($p < 0.001$ versus SCI and Sham) and callus porosity ($p = 0.04$ versus Sham and $p = 0.002$ versus SCI) (Table 1).

LIPUS strengthened the non-fractured tibia and bone callus in SCI rats

Our mechanical test evidenced that LIPUS effectively counteracted the deleterious effects of SCI on tibial bone strength (Table 2). SCI rats exhibited significantly weaker bones than the Shams, whence the maximal load was decreased by 55% ($p = 0.0004$) and the stiffness by 50% ($p = 0.0009$). Conversely, LIPUS significantly increased stiffness by 89% compared to the non-treated SCI rats ($p = 0.002$) and reached values statistically similar to those in the Sham group ($p = 0.87$). Although not significantly, LIPUS also increased the maximal load by 16% compared to the non-treated SCI rats ($p = 0.14$), but values remained different than Sham rats ($p = 0.0001$). Regarding the bone callus, LIPUS was also effective at ameliorating the loss of strength induced by the paraplegia. As of note, SCI impaired bone callus mechanical integrity by reducing the maximal torque in 44%, $p = 0{,}0008$, energy in 54%, $p = 0.003$, and ultimate angle in 62%, $p = 0.001$, in comparison with sham. LIPUS, on the other hand, significantly increased peak torque by 88% ($p = 0.0006$) and ultimate angle by 90% ($p = 0.017$) compared to the non-treated SCI rats, reaching values comparable to those in the Sham group ($p = 0.3$ and $p = 0.1$, respectively).

DISCUSSION

Bone is a tissue in constant activity, being constantly remodeled by a balanced formation and resorption activity. During fracture repair, each stage is influenced by the previous one, ultimately aimed at the union of the fractured fragments and recovering the mechanical and biological properties of the bone [17]. The repair cascade comprises an anabolic stage, in which bone and cartilage are formed, and a catabolic stage, in which the cartilage is replaced by bone, which, in turn, is remodeled to restore normal bone structure [18]. Several diseases and conditions are known to impair bone activity. In this study, we reported a considerable impairment in the quality of non-fracture bones as well in the bone callus formation due to a complete injury at the spinal cord [8].

Osteoporosis corresponds to a progressive systematic skeletal disease, characterized by low bone mass, microarchitectural deterioration, with a consequent increase in bone fragility and fracture risk. Specifically, the term disuse osteoporosis refers to bone losses due to reductions in mechanical loading. Although several conditions are associated with disuse osteoporosis (i.e., spaceflight exposure, long-term bed rest, and para- or quadriplegia), the underlying mechanisms, aetiologies, and bone phenotypes may vary considerably across these unloading models [19]. Bone loss following SCI is certainly unique in its magnitude and rapidity, which may be explained by the absence of mechanical loading in response to motor dysfunction, combined with muscle atrophy, post-injury neurogenic, vascular, neural, and endocrine changes [20]. Cellularly, bone disuse due to SCI leads to an increase in osteoclast activity and a reduction in osteoblast and osteocyte function [21]. The highly uncoupled bone turnover due to SCI, associated with the above disorders, potentially increases low impact fracture risk in these individuals. Different than general osteoporosis, SCI-induced osteoporosis is more prevalent in sublesional bones, especially distal femur and proximal tibia. Likewise, the specific SCI-induced bone loss risk factors include motor complete lesions, and duration of injury, differing from the risk factors for general osteoporosis, such as white race, female gender, prevalent fractures, low body mass index, and family history of fractures [22].

Several procedures can positively interfere with bone callus formation, in which bone graft is the first and oldest among them, followed by alternatives to grafts (i.e., hydroxyapatite and calcium carbonate) [23, 24]. Biophysical methods may also be used for fracture repair, including electromagnetic fields and low-intensity pulsed ultrasound [25]. The first report of LIPUS as a clinical approach to accelerate fracture healing in patients was in 1983 [13]. Based on the patient analysis, the use of LIPUS was approved by the US Food and Drug Administration (FDA) [26]. This led us to investigate the effects of LIPUS treatment on bone quality and callus formation. Indeed, we have detected a promising osteogenic effect of LIPUS as an approach to restore bone and callus quality in SCI rats.

There is clinical evidence in humans that the use of LIPUS accelerates bone callus formation [27] and generates positive outcomes for the treatment of pseudoarthrosis and other bone consolidation defects [7]. In fact, recent meta-analyses proved the efficiency of LIPUS in treating not only delayed and nonunion fractures [28], but also fresh fractures [29].

Table 1. Assessment of bone density by DXA, and bone microarchitecture by μCT.

	Sham	SCI	SCI + US
DXA at tibia			
BMD (g/cm²)	0.07 ± 0.01	0.04 ± 0.008[a]	0.05 ± 0.009[a]
BMC (g)	0.006 ± 0.001	0.003 ± 0.001[a]	0.004 ± 0.001[a]
DXA at callus			
BMD (g/cm²)	0.17 ± 0.01	0.11 ± 0.02[a]	0.13 ± 0.02[a,b]
BMC (g)	0.07 ± 0.01	0.05 ± 0.007[a]	0.06 ± 0.012
Area (cm^2)	0.40 ± 0.07	0.45 ± 0.07	0.46 ± 0.10
μCT at trabecular bone			
BV (mm^3)	3.19 ± 1.86	0.70 ± 0.40[a]	0.55 ± 0.30[a]
BV/TV (%)	6.68 ± 4.57	1.81 ± 1.02[a]	1.44 ± 0.80[a]
Tb.Th (mm)	0.05 ± 0.004	0.04 ± 0.004[a′]	0.05 ± 0.001
Tb.N (mm)	1.22 ± 0.86	0.39 ± 0.23[a]	0.31 ± 0.17[a]
Tb.Sp (mm)	0.61 ± 0.34	1.10 ± 0.21[a]	1.25 ± 0.37[a]
TMD (g/cm^3)	0.30 ± 0.05	0.27 ± 0.01	0.28 ± 0.01
Conn.D (1/mm)	74.61 ± 68.75	23.85 ± 8.19[a′]	24.48 ± 15.80[a]
BS/BV (mm)	86.97 ± 3.40	94.81 ± 10.46	90.05 ± 5.43
μCT at cortical bone			
Ct.V	7.51 ± 0.67	5.01 ± 0.52[a]	6.39 ± 0.29[a,b]
Ct.BV/TV (%)	70.03 ± 2.97	58.39 ± 5.97[a]	67.18 ± 4.85[b]
Ct.Th (mm)	0.25 ± 0.05	0.22 ± 0.03	0.25 ± 0.03
TMD (g/cm^3)	0.35 ± 0.03	0.32 ± 0.01[a′]	0.34 ± 0.01
μCT at callus			
Ca.V (mm^3)	30.34 ± 7.56	25.38 ± 5.79	33.89 ± 12.55
Ca.BV/TV (%)	22.82 ± 2.81	24.06 ± 5.16	30.39 ± 6.35[a,b′]
Tb.Th (mm)	0.08 ± 0.009	0.07 ± 0.005[a]	0.07 ± 0.005[a,b′]
Tb.N (mm)	2.55 ± 0.45	2.98 ± 0.30	4.34 ± 0.86[a,b]
Tb.Sp (mm)	0.25 ± 0.04	0.26 ± 0.05	0.13 ± 0.02[a,b]
Ca.TMD (g/cm^3)	0.06 ± 0.04	0.08 ± 0.06	0.24 ± 0.15[a]
Conn.D (1/mm)	285.75 ± 38.70	274.90 ± 23.29	763.87 ± 81.96[a,b]
Ca.Po (%)	76.07 ± 1.86	80.08 ± 2.18[a]	69.60 ± 6.35 [a,b]

Values are means ± standard deviation, $n = 6$/group.
[a]$p < 0.05$ versus Sham.
[a′]$p < 0.09$ versus Sham.
[b]$p < 0.05$ versus SCI.
[b′]$p < 0.09$ versus SCI.

Experimentally, Cheung investigated the effects of LIPUS on an ovariectomy-induced osteoporotic fracture rat model. The authors evidenced upregulation of Col-1, bone morphogenetic protein–2, vascular endothelial growth factor, and osteoprotegerin post-fracture in rats treated with LIPUS, leading to higher callus formation at weeks 2–4 with enhanced endochondral ossification [8]. Indeed, some mechanisms of how LIPUS stimulated bone healing were postulated; the increased angiogenesis rate [30, 31], fibroblast and vascular endothelial growth factors [32, 33], proteoglycan, nitric oxide, and prostaglandin E2 synthesis [34, 35], platelet-derived factor synthesis, and aggrecan messenger RNA expression [36, 37]. Tang et al. also conducted a study to investigate the effects of LIPUS on bone healing in OVX rats, and suggested a crucial role of MSTN signal pathways in enhanced bone healing due to LIPUS treatment [38]. In a recent study, Shimizu et al. highlighted the essential role of osteocytes in promoting bone healing during LIPUS stimulation in two different in vivo models. The authors detected that LIPUS accelerated fracture healing in zebrafish, whose bone has osteocytes, but not in medaka, whose bone does not have osteocytes [39].

To our knowledge, our study was the first to investigate the effects of LIPUS in an SCI-induced bone loss rat model, with severe osteoporosis and poor callus formation. Our results suggest that LIPUS effectively counteracted the effects of bone loss induced by SCI in non-fractured bones and bone healing in fracture callus. Interestingly, at the fracture callus, the stimulated tissue is in the near field (nearby transducer), but tibias are in the far field, and yet we reported positive osteogenic activation due to LIPUS. Accordingly, Fung et al. have shown pressure variations in the near field (nearby transducer) and uniform profile in the far field [40].

Although the exact mechanisms underlying the osteogenic effects of LIPUS on bone metabolism and fracture healing remain unclear, the RANKL/RANK/OPG system seems to play an important role in this process [41]. The RANKL is released by osteoblast lineage cells and binds to its receptor RANK on the surface of myeloid cells, stimulating their differentiation into osteoclasts [42]. The OPG, produced by osteoblasts, is a decoy receptor for RANKL, which blocks the RANKL-RANK interaction by binding to RANKL, thus inhibiting osteoclast formation and bone resorption [43]. In unloading conditions, the source of RANKL was revealed to be

Table 2. Assessment of bone strength by mechanical test.

	Sham	SCI	SCI + US
Mechanical test at tibia			
Maximal load (N)	53.40 ± 7.80	29.50 ± 2.07[a]	34.34 ± 4.7
Stiffness (N.mm)	143.54 ± 12.80	71.05 ± 26.36[a]	134.21 ± 25.97[b]
Energy (N.m)	3.70 ± 2.48	1.94 ± 0.94	2.15 ± 0.88
Mechanical test at callus			
Peak torque (N.m)	0.09 ± 0.01	0.05 ± 0.01[a]	0.09 ± 0.01[b]
Ultimate angle (deg)	44.51 ± 13.32	16.98 ± 12.38[a]	32.18 ± 11.87[b]
Energy (N.m/deg)	0.0009 ± 0.0006	0.0004 ± 0.0005[a]	0.0005 ± 0.0001
Stiffness (N.mm/deg)	7.07 ± 1.31	4.71 ± 2.56	7.82 ± 3.06

SCI significantly impaired the maximal load and stiffness of the non-fractured tibias when compared to the Shams. Similarly, SCI also decreased peak torque, ultimate angle, and energy of the fractured callus when compared to the Shams. LIPUS fully restored the stiffness of the non-fractured tibias, and the peak torque and ultimate angle of the callus to values comparable to the Shams. Values are means ± standard deviation, $n = 6$/group.
[a]$p < 0.05$ versus Sham.
[b]$p < 0.05$ versus SCI.

osteocytes [44], reflecting its fundamental role in mechanotransduction. Although a major signaling pathway of mechanosensors remains to be elucidated, the RANKL/RANK/OPG axis seems to play a critical role in preventing bone loss and healing impair in LIPUS-treated SCI rats. A recent study supports this idea, in which the authors documented the regulation of RANKL expression by mechanosensing and mechanotransduction [44]. Likewise, previous authors evidenced an in vitro increase in mRNA expression of RANKL and OPG six hours after LIPUS treatment, with a further increase of OPG mRNA expression after 12 h. These findings were also confirmed by in vivo study with goldfish, in which the osteoclastic marker enzymes tended to decrease two weeks after daily LIPUS, while osteoblastic marker enzymes were activated [45].

In our study, LIPUS was effective at partially restoring endochondral ossification at the femoral callus, increasing collagen deposition and OPG-positive-area, decreasing resorptive area, leading to higher density and improved microarchitecture, ultimately resulting in stronger fracture callus. At the tibias, LIPUS normalized the osteoblastic-related gene expression, decreased resorptive area, increased trabecular area, and decreased RANK and RANK-L-positive areas, leading to higher cortical volume and stronger tibias. Fung et al. also demonstrated bone changes due to the far field ultrasound waves [40]. The authors concluded that axial distance beyond near field could transmit ultrasound energy to osteocytes more efficiently and promote mechanotransduction between osteocytes and osteoblasts via paracrine factors secretion. Therefore, LIPUS was either partially or fully capable of reversing unfavorable bone loss and callus changes in cases of severe osteoporosis.

It is important to highlight that LIPUS was initiated ten days after spinal cord injury in this study, during the onset of bone loss. Therefore, caution is needed when concluding whether LIPUS reverted the SCI-bone loss or decrease the acute loss following injury. Either way, our findings are sufficient to infer the osteogenic effects of LIPUS on both the fracture healing and non-fractured tibias. Another important aspect that needs to be discussed in this study is related to the ultrasound transducer dimension and its proportion to the femur and tibia in rodents versus humans. Considering that the transducer measures 20 mm in diameter, and the average length for femurs and tibias are 41 mm and 46 mm, respectively, we confirm that the osteogenic effects detected at the tibias were due to the far field ultrasound waves, and not a direct application. However, we may keep in mind that the distance from the transducer to the rat's proximal metaphyseal tibias is roughly 15 mm, and this should be considered when extrapolating these findings into human clinical practices.

In conclusion, therapeutic LIPUS partially reversed the deleterious changes in non-fractured tibias and femoral bone callus formation after SCI. At the tibias, LIPUS counteracted the SCI-induced bone loss effects by simultaneously increasing bone formation and decreasing bone resorption. We also evidenced the osteogenic effects of LIPUS at partially restoring the endochondral ossification during callus formation, leading to a newly formed tissue with improved microarchitecture and mechanical integrity. Therefore, LIPUS may be an efficient and non-invasive approach to prevent bone loss and osteoporotic fracture in SCI individuals.

DATA AVAILABILITY

The datasets generated during and/or analyzed during the current study are available from the corresponding author on reasonable request. All data generated or analyzed during this study are included in this published article.

REFERENCES

1. Cruz CD, Coelho A, Antunes-Lopes T, Cruz F. Biomarkers of spinal cord injury and ensuing bladder dysfunction. Adv Drug Deliv Rev. 2015;82-83:153–9.
2. Ozisler Z, Koklu K, Ozel S, Unsal-Delialioglu S. Outcomes of bowel program in spinal cord injury patients with neurogenic bowel dysfunction. Neural Regen Res. 2015;10:1153–8. https://pubmed.ncbi.nlm.nih.gov/26330842.
3. Hoh DJ, Mercier LM, Hussey SP, Lane MA. Respiration following spinal cord injury: evidence for human neuroplasticity. Respir Physiol Neurobiol. 2013;189:450–64. https://pubmed.ncbi.nlm.nih.gov/23891679.
4. Bauman WA, Spungen AM. Coronary heart disease in individuals with spinal cord injury: assessment of risk factors. Spinal Cord. 2008;46:466–76. https://doi.org/10.1038/sj.sc.3102161.
5. Kovindha A, Kammuang-Lue P, Prakongsai P, Wongphan T. Prevalence of pressure ulcers in Thai wheelchair users with chronic spinal cord injuries. Spinal Cord. 2015;53:767–71. https://pubmed.ncbi.nlm.nih.gov/25939607.
6. Abdelrahman S, Ireland A, Winter EM, Purcell M, Coupaud S. Osteoporosis after spinal cord injury: aetiology, effects and therapeutic approaches. J Musculoskelet Neuronal Interact. 2021;21:26–50. http://www.ncbi.nlm.nih.gov/pubmed/33657753.
7. Hadjiargyrou M, McLeod K, Ryaby JP, Rubin C. Enhancement of fracture healing by low intensity ultrasound. Clin Orthop Relat Res. 1998;355S:S216–29. https://doi.org/10.1097/00003086-199810001-00022.
8. Cheung W-H, Chow SK, Sun M-H, Qin L, Leung K-S. Low-Intensity pulsed ultrasound accelerated callus formation, angiogenesis and callus remodeling in osteoporotic fracture healing. Ultrasound Med Biol. 2011;37:231–8. https://doi.org/10.1016/j.ultrasmedbio.2010.11.016.
9. Lewis DI. Animal experimentation: implementation and application of the 3Rs. Willmott C, editor. Emerg Top Life Sci. 2019;3:675–9. https://portlandpress.com/emergtoplifesci/article/3/6/675/220907/Animal-experimentation-implementation-and.
10. Guide for the Care and Use of Laboratory Animals. Guide for the care and use of laboratory animals. 2011. http://www.ncbi.nlm.nih.gov/pubmed/21595115.

11. Butezloff MM, Volpon JB, Ximenez JPB, Astolpho K, Correlo VM, Reis RL, et al. Gene expression changes are associated with severe bone loss and deficient fracture callus formation in rats with complete spinal cord injury. Spinal Cord. 2019:58:365–76.
12. Santiago HAR, Zamarioli A, Sousa Neto MD, Volpon JB. Exposure to secondhand smoke impairs fracture healing in rats. Clin Orthop Relat Res. 2017;475:903–5.
13. Duarte LR. The stimulation of bone growth by ultrasound. Arch Orthop Trauma Surg. 1983;101:153–9. https://doi.org/10.1007/bf00436764.
14. Bouxsein ML, Boyd SK, Christiansen BA, Guldberg RE, Jepsen KJ, Muller R, et al. Guidelines for assessment of bone microstructure in rodents using micro-computed tomography. J Bone Min Res. 2010;25:1468–86. https://www.ncbi.nlm.nih.gov/pubmed/20533309.
15. Zamarioli A, Campbell ZR, Maupin KA, Childress PJ, Ximenez JPB, Adam G, et al. Analysis of the effects of spaceflight and local administration of thrombopoietin to a femoral defect injury on distal skeletal sites. NPJ Microgravity. 2021;7:12. http://www.ncbi.nlm.nih.gov/pubmed/33772025.
16. Chakraborty N, Zamarioli A, Gautam A, Campbell R, Mendenhall SK, Childress PJ. et al. Gene-metabolite networks associated with impediment of bone fracture repair in spaceflight. Comput Struct Biotechnol J. 2021;19:3507–20. https://pubmed.ncbi.nlm.nih.gov/34194674.
17. Glatt V, Evans CH, Tetsworth K. A concert between biology and biomechanics: the influence of the mechanical environment on bone healing. Front Physiol. 2017;7:678 https://pubmed.ncbi.nlm.nih.gov/28174539.
18. Hankenson KD, Zimmerman G, Marcucio R. Biological perspectives of delayed fracture healing. Injury. 2014;45:S8–15. https://pubmed.ncbi.nlm.nih.gov/24857030.
19. Giangregorio L, Blimkie CJR. Skeletal adaptations to alterations in weight-bearing activity: a comparison of models of disuse osteoporosis. Sports Med. 2002;32:459–76. http://www.ncbi.nlm.nih.gov/pubmed/12015807.
20. Haider IT, Lobos SM, Simonian N, Schnitzer TJ, Edwards WB. Bone fragility after spinal cord injury: reductions in stiffness and bone mineral at the distal femur and proximal tibia as a function of time. Osteoporos Int. 2018;29: 2703–2715.
21. Sahbani K, Cardozo CP, Bauman WA, Tawfeek HA. Inhibition of TGF-β signaling attenuates disuse-induced trabecular bone loss after spinal cord injury in male mice. Endocrinology. 2022;163. https://academic.oup.com/endo/article/doi/10.1210/endocr/bqab230/6427655.
22. Wilmet E, Ismail AA, Heilporn A, Welraeds D, Bergmann P. Longitudinal study of the bone mineral content and of soft tissue composition after spinal cord section. Paraplegia. 1995;33:674–7.
23. Giannoudis PV, Jones E, Einhorn TA. Fracture healing and bone repair. Injury. 2011;42:549–50. https://www.ncbi.nlm.nih.gov/pubmed/21474131.
24. Dimitriou R, Jones E, McGonagle D, Giannoudis PV. Bone regeneration: current concepts and future directions. BMC Med. 2011;9:66. http://www.ncbi.nlm.nih.gov/pubmed/21627784.
25. Schandelmaier S, Kaushal A, Lytvyn L, Heels-Ansdell D, Siemieniuk RAC, Agoritsas T, et al. Low intensity pulsed ultrasound for bone healing: systematic review of randomized controlled trials. BMJ. 2017;356:j656. http://www.ncbi.nlm.nih.gov/pubmed/28348110.
26. Harrison A, Alt V. Low-intensity pulsed ultrasound (LIPUS) for stimulation of bone healing – a narrative review. Injury. 2021;52:S91–6. https://doi.org/10.1016/j.injury.2021.05.002.
27. Pounder NM, Harrison AJ. Low intensity pulsed ultrasound for fracture healing: a review of the clinical evidence and the associated biological mechanism of action. Ultrasonic. 2008;48:330–8. https://doi.org/10.1016/j.ultras.2008.02.005.
28. Leighton R, Watson JT, Giannoudis P, Papakostidis C, Harrison A, Steen RG, et al. Healing of fracture nonunions treated with low-intensity pulsed ultrasound (LIPUS): a systematic review and meta-analysis. Injury. 2017;48:1339–47. https://doi.org/10.1016/j.injury.2017.05.016. Available from
29. Bashardoust Tajali S, Houghton P, MacDermid JC, Grewal R. Effects of low-intensity pulsed ultrasound therapy on fracture healing. Am J Phys Med Rehabil. 2012;91:349–67. https://doi.org/10.1097/phm.0b013e31822419ba.
30. Yang KH, Parvizi J, Wang SJ, Lewallen DG, Kinnick RR, Greenleaf JF, et al. Exposure to low-intensity ultrasound increases aggrecan gene expression in a rat femur fracture model. J Orthop Res. 1996;14:802–9. http://www.ncbi.nlm.nih.gov/pubmed/8893775.
31. Zhou X-Y, Wu S-Y, Zhang Z-C, Wang F, Yang Y-L, Li M, et al. Low-intensity pulsed ultrasound promotes endothelial cell-mediated osteogenesis in a conditioned medium coculture system with osteoblasts. Medicine. 2017;96:e8397. http://www.ncbi.nlm.nih.gov/pubmed/29069035.
32. Wang F-S, Kuo Y-R, Wang C-J, Yang KD, Chang P-R, Huang Y-T, et al. Nitric oxide mediates ultrasound-induced hypoxia-inducible factor-1alpha activation and vascular endothelial growth factor-A expression in human osteoblasts. Bone. 2004;35:114–23. http://www.ncbi.nlm.nih.gov/pubmed/15207747.
33. Hiyama A, Mochida J, Iwashina T, Omi H, Watanabe T, Serigano K, et al. Synergistic effect of low-intensity pulsed ultrasound on growth factor stimulation of nucleus pulposus cells. J Orthop Res. 2007;25:1574–81. http://www.ncbi.nlm.nih.gov/pubmed/17593536.
34. Reher P, Doan N, Bradnock B, Meghji S, Harris M. Effect of ultrasound on the production of IL-8, basic FGF and VEGF. Cytokine. 1999;11:416–23. http://www.ncbi.nlm.nih.gov/pubmed/10346981.
35. Reher P, Harris M, Whiteman M, Hai HK, Meghji S. Ultrasound stimulates nitric oxide and prostaglandin E2 production by human osteoblasts. Bone. 2002;31:236–41. http://www.ncbi.nlm.nih.gov/pubmed/12110440.
36. Borovecki F, Pecina-Slaus N, Vukicevic S. Biological mechanisms of bone and cartilage remodelling-genomic perspective. Int Orthop. 2007;31:799–805. http://www.ncbi.nlm.nih.gov/pubmed/17609952.
37. Ito M, Azuma Y, Ohta T, Komoriya K. Effects of ultrasound and 1,25-dihydroxyvitamin D3 on growth factor secretion in co-cultures of osteoblasts and endothelial cells. Ultrasound Med Biol. 2000;26:161–6. http://www.ncbi.nlm.nih.gov/pubmed/10687804.
38. Tang L, Kang Y, Sun S, Zhao T, Cao W, Fan X, et al. Inhibition of MSTN signal pathway may participate in LIPUS preventing bone loss in ovariectomized rats. J Bone Min Metab. 2019;38:14–26. https://doi.org/10.1007/s00774-019-01029-5.
39. Shimizu T, Fujita N, Tsuji-Tamura K, Kitagawa Y, Fujisawa T, Tamura M, et al. Osteocytes as main responders to low-intensity pulsed ultrasound treatment during fracture healing. Sci Rep. 2021;11:10298. https://pubmed.ncbi.nlm.nih.gov/33986415.
40. Fung C-H, Cheung W-H, Pounder NM, Harrison A, Leung K-S. Osteocytes exposed to far field of therapeutic ultrasound promotes osteogenic cellular activities in pre-osteoblasts through soluble factors. Ultrason. 2014;54:1358–65. https://doi.org/10.1016/j.ultras.2014.02.003.
41. Gifre L, Ruiz-Gaspà S, Carrasco JL, Portell E, Vidal J, Muxi A, et al. Effect of recent spinal cord injury on the OPG/RANKL system and its relationship with bone loss and the response to denosumab therapy. Osteoporos Int. 2017;28:2707–15. http://link.springer.com/10.1007/s00198-017-4090-4.
42. Trang NM, Kim E-N, Lee H-S, Jeong G-S. Effect on osteoclast differentiation and ER stress downregulation by amygdalin and RANKL binding interaction. Biomolecules. 2022. http://www.ncbi.nlm.nih.gov/pubmed/35204757.
43. Yao Z, Getting SJ, Locke IC. Regulation of TNF-induced osteoclast differentiation. Cells. 2021;11. http://www.ncbi.nlm.nih.gov/pubmed/35011694.
44. Sasaki F, Hayashi M, Ono T, Nakashima T. The regulation of RANKL by mechanical force. J Bone Min Metab. 2021;39:34–44. https://link.springer.com/10.1007/s00774-020-01145-7.
45. Hanmoto T, Tabuchi Y, Ikegame M, Kondo T, Kitamura K-I, Endo M, et al. Effects of low-intensity pulsed ultrasound on osteoclasts: Analysis with goldfish scales as a model of bone. Biomed Res. 2017;38:71–7. http://www.ncbi.nlm.nih.gov/pubmed/28239034.

ACKNOWLEDGEMENTS

We would like to thank all the investigators, staff, and trainees from the Laboratory of Bioengineering at the School of Medicine of Ribeirão Preto, University of São Paulo, Brazil, who assisted in the entire study. We also would like to thank the 3B's Research Group (Portugal) as well as the School of Dentistry of Ribeirão Preto, University of São Paulo, Brazil, who assisted in the microstructural analysis. The São Paulo Research Foundation funded this study (FAPESP) - 2015/22126-1.

COMPETING INTERESTS

The authors declare no competing interests.

ETHICS

We certify that all applicable institutional and governmental regulations concerning the ethical use of animals were followed during the course of this research.

ADDITIONAL INFORMATION

Correspondence and requests for materials should be addressed to Ariane Zamarioli.